Desalination and Water Treatment
www.deswater.com

doi:10.5004/dwt.2017.0015

100 (2017) 67–74
December

Adsorption of fluoride from aqueous solution on supported Fe/γ-Al_2O_3 adsorbent prepared by ultrasonic-assisted technique

Yong Liu[a,b,*], Shixiang Wang[a], Qin Fan[a], Yanlan Liu[a], Wenhui Zhou[a]

[a]*College of Chemistry and Materials Science, Sichuan Normal University, Chengdu 610066, China, email: liuyongsicnu@sina.com (Y. Liu) , 454180602@qq.com (S.X. Wang), 960345742@qq.com (Q. Fan), 360124586@qq.com (Y.L. Liu), 1773917113@qq.com (W.H. Zhou)*

[b]*Key Laboratory of Treatment for Special Wastewater of Sichuan Province Higher Education System, Sichuan, Chengdu 610066, China*

Received 6 January 2016; Accepted 10 June 2016

ABSTRACT

A novel adsorbent (Fe/γ-Al_2O_3) was successfully synthesized by ferrous sulfate impregnating γ-Al_2O_3 under ultrasonic condition to remove fluoride from aqueous solutions. The adsorbent was characterized by the X-ray diffraction, transmission electron microscopy, X-ray photoelectron spectroscopy and Brunauer–Emmett–Teller. The fluoride adsorption behavior of Fe/γ-Al_2O_3 was studied with the help of different process parameters vs. contact time, initial fluoride concentration, initial pH and other co-ions effect. Maximum magnitude of fluoride was adsorbed from aqueous solution at initial pH 5.5. Coexistence of SO_4^{2-}, NO_3^- and Cl^- did not affect fluoride adsorption, and high concentrations of HCO_3^- or PO_4^{3-} only led to partial inhibition of fluoride adsorption. Adsorption kinetic study revealed that the adsorption process followed pseudo-second-order model. Adsorption data were fitted to Langmuir isotherm model, and the adsorption capacity was found to be 1.65 mg g^{-1}. A high desorption efficiency of 96.7% was achieved by treating fluoride loaded Fe/γ-Al_2O_3 with 0.50 M NaOH solution. In addition, the adsorption mechanism analysis revealed that the pH variation during the adsorption of fluoride was mainly resulted from that the hydroxyl groups on the surface of the Fe/γ-Al_2O_3 with amphoteric behavior in solution reacted with fluoride anions.

Keywords: Supported Fe/γ-Al_2O_3 adsorbent; Ultrasonic wave; Fluoride; Adsorption isotherms; Adsorption kinetics

1. Introduction

Fluoride is a persistent and non-degradable toxin that accumulates in soil, plants, water, wildlife and humans [1]. Elevated fluoride concentrations in the groundwater were found in various parts of the world [2]. Groundwater is a major source of human intake of fluoride. Besides the natural geological sources (e.g., geochemical reactions and volcanic emissions), industries discharges (e.g., semiconductor, electroplating, steel and fertilizer industries) are also major sources of fluoride pollution in groundwater [3,4].

Excess fluoride in drinking water causes harmful effects such as dental and skeletal fluorosis, and it can also inhibit the regenerative functions of animals and the growth of plants [5,6]. The World Health Organization has set a guidance value of 1.5 mg L^{-1} for fluoride in drinking water, and the corresponding Chinese drinking water standard is 1.0 mg L^{-1}. The Chinese wastewater first-level effluent standard for fluoride has been specified as 10 mg L^{-1} [7–9]. For these reasons, the removal of the excess fluoride from waters and wastewaters is important in terms of protecting public health and environment.

Many methods have been developed for fluoride removal from water, such as precipitation, membrane processes, ion exchange and adsorption processes [10,11]. Adsorption is

---

*Corresponding author.

Presented at the 6th IWA-ASPIRE Conference & Exhibition, Beijing, China, 20–24 September 2015.

one of the most useful and economical techniques for the removal of pollutant with low concentrations [3,12]. Among all of the defluoridation adsorbents, activated alumina is the most commonly used one due to its large specific surface area, abundance of surface functional groups, wide pore size distribution and good mechanical robustness [13]. Nevertheless, when activated alumina is applied for fluoride removal, its low adsorption capacity necessitates the use of large quantities and frequent regeneration, which causes high operating cost [14,15].

In recent years, considerable attention has been devoted to the development of effective fluoride removal materials. In this context, alumina has been modified by using various materials to improve the fluoride removal efficiency [3]. Iron ion is classified into a hard acid ion which has strong affinity toward fluoride ion and is often used to remove fluoride. Therefore, the composite of iron and aluminum with more active site show considerable enhancement of fluoride adsorption capacities [1]. However, to the best of our knowledge, these composite of iron and aluminum were mainly prepared by common dipping method, co-precipitation method and sol-gel method. Studies of the behavior of supported γ-Al_2O_3 adsorbents obtained by sonication-assisted synthesis in the presence of fluoride ion are limited. With sonication-assisted precipitation, both dispersion and size of the particles can be tailored. It has been confirmed in the synthesis of materials [16,17]. Therefore, the iron supported γ-Al_2O_3 adsorbent obtained by sonication-assisted synthesis seems to be an alternative for efficient fluoride removal due to its better dispersion of iron particles.

In the present study, we have successfully developed a new adsorbent by impregnation of γ-Al_2O_3 with iron salts at sonication-assisted condition to remove fluoride from aqueous solution. Batch studies were conducted using these novel adsorbents with optimization of various experimental conditions, including contact time, adsorbent dose, initial pH and co-existing ions in solutions. The nature and morphology of the adsorbents were therefore discussed on the basis of X-ray diffraction (XRD), X-ray photoelectron spectroscopy (XPS), transmission electron microscopy (TEM) and Brunauer–Emmett–Teller (BET) studies. The Langmuir and Freundlich isotherm models were used to explain the mechanism of fluoride removal by this novel adsorbent. Various kinetic models were also included to describe the adsorption process.

2. Materials and methods

2.1. Materials and preparation of adsorbent

The plain γ-Al_2O_3 (particle size was less than 3 mm) was obtained from Ruilong Wastewater Treatment Materials Company (China), and $FeSO_4·7H_2O$ (reagent grade) was provided by Shanghai Chemical Reagents Company (China). 10 g of plain γ-Al_2O_3 particles were dispersed in a ferrous sulfate solution (250 mL, 72 mmol L^{-1}) under ultrasonication with the ultrasonic wave power of 250 W for 15 min. The resulting solid particles were separated from the solution with a filter method and washed with distilled water for several times until no iron ion was tested and vacuum-dried at 105°C for 24 h. The samples were then naturally cooled to room temperature, and the resulting products were denoted as Fe/γ-Al_2O_3. The plain γ-Al_2O_3 and Fe/γ-Al_2O_3 were characterized by XRD (model XD-2, Beijing, China), TEM (JEOL2010, Japan) and XPS (KRATOS XSAM-800, Japan) analyses. The surface area of the new the plain γ-Al_2O_3 and Fe/γ-Al_2O_3 were measured by BET surface area analyzer (Micromeritics TriStar Surface Area and Porosity Analyzer, nitrogen absorption apparatus, America).

2.2. Adsorption experiments

Stock solution of 100 mg L^{-1} fluoride concentration was prepared by dissolving 0.221 g NaF in 1 L distilled water. Experimental solutions of the desired concentrations were obtained by successive dilution of the stock solution.

The effect of initial pH on fluoride adsorption was investigated by adjusting the initial solution pH from 1 to 11 using 0.1 mol L^{-1} HCl and 0.1 mol L^{-1} NaOH with an initial fluoride concentration of 30 mg L^{-1} and with 50 g L^{-1} of adsorbent. The experiments were carried out in polypropylene flasks containing 100 mL of fluoride solution and 5 g of adsorbent, and then, the mixed suspensions were shaken at 150 rpm in a shaker at ambient temperature (25±1°C) for 24 h; after the above steps, the adsorbent was separated from the solution by centrifugation, and the residual fluoride concentration in solution was measured by the fluoride ion selective electrode (Rex Electric Chemical, pF-1)

The effects of co-existing anions (PO_4^{3-}, SO_4^{2-}, HCO_3^-, NO_3^- and Cl^-) on fluoride removal were performed with an adsorbent dose of 50 g L^{-1} and an initial fluoride concentration of 30 mg L^{-1}. The co-existing anions were set at fixed concentration of 100 mg L^{-1}, respectively. Other procedures were as same as the steps of study for pH effect.

The adsorption isotherm experiments were carried out at pH of 6.0. The initial fluoride concentration was varied from 10 to 200 mg L^{-1}. In each test, 5 g adsorbent was added into 100 mL fluoride solutions with different initial concentrations. The solution pH was controlled as constant by adjusting a certain amount of HCl and/or NaOH during the adsorption process. Other procedures were as the same as the steps of study for pH effect.

In the kinetics study, the volume of the solution was 300 mL, and the initial fluoride concentrations were 30 mg L^{-1}. The adsorbent dose was 15 g, and the solution pH value was controlled at 6.0. During the experiment, the water samples were taken at different time intervals for the determination of fluoride concentrations. Other procedures were as the same as the steps of study for pH effect.

In the regeneration study, the spent adsorbent was first separated through centrifuge and washed by deionized water for several times. 26.5 mg of fluoride bearing sample was taken into polypropylene bottles with 30 mL of NaOH solution. Different concentrations NaOH solution were chosen as an elution solution, and desorption time was 6 h. The adsorption study was as the same as the above.

The amount of fluoride adsorbed per unit weight of adsorbent at time t, q_t (mg g^{-1}) and fluoride removal efficiency, R, were calculated as follows:

$$q_t = \frac{(C_0 - C_t) \times V}{M} \tag{1}$$

$$R = \frac{(C_0 - C_t) \times 100}{C_0} \tag{2}$$

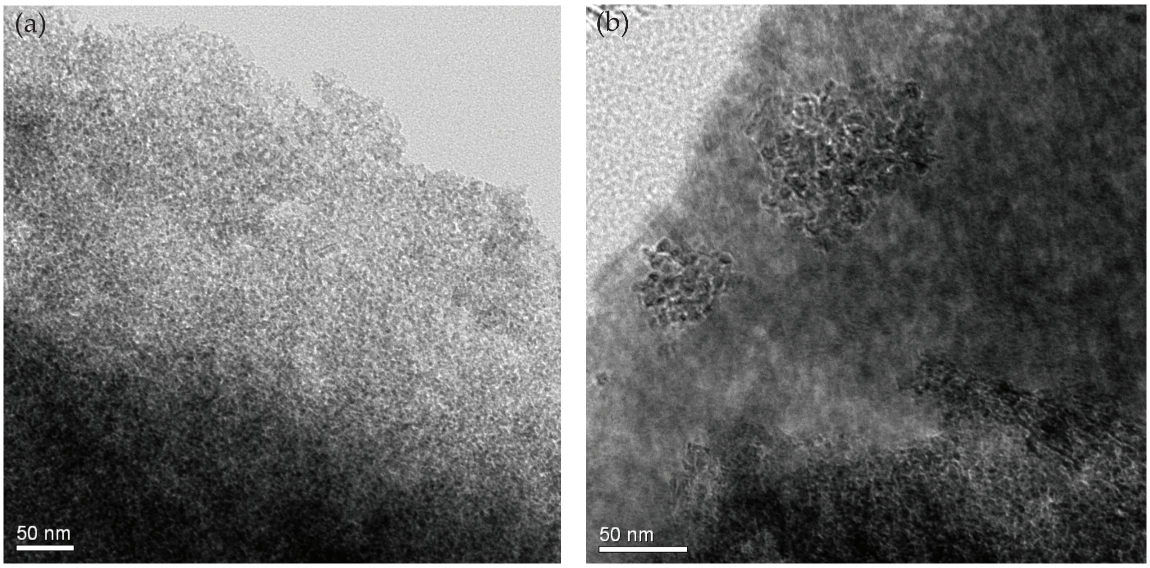

(a) TEM image of γ-Al_2O_3 (b) TEM image of Fe/γ-Al_2O_3

Fig. 1. TEM images of γ-Al_2O_3 and Fe/γ-Al_2O_3.

where C_0 is initial concentrations of fluoride, C_t is concentration of fluoride at any time, M is the mass of adsorbent (g) and V is the volume of the solution (L).

3. Results and discussion

3.1. Characterization of materials

The adsorbent was characterized to study its surface area and pore volume. It was found that the main pore volumes of Fe/γ-Al_2O_3 and plain γ-Al_2O_3 were 0.341 and 0.356 $cm^3\ g^{-1}$, respectively, while their BET surface areas were found to be about 304.3 and 320.0 $m^2\ g^{-1}$, respectively. The lower specific surface area of Fe/γ-Al_2O_3 may be due to the severe aggregation of iron oxide layers.

The surface morphology of γ-Al_2O_3 and Fe/γ-Al_2O_3 was characterized by TEM. As shown in Fig. 1(a), γ-Al_2O_3 has a regular form. The Fe/γ-Al_2O_3 sample was opaque, and some amorphous particles scattered on the surface of Fe/γ-Al_2O_3 (Fig. 1(b)) was probably due to the presence of iron compounds on the γ-Al_2O_3.

The XRD patterns of Fe/γ-Al_2O_3 and plain γ-Al_2O_3 in Fig. 2 confirmed the amorphous nature of the Fe/γ-Al_2O_3 material. The pattern of pure γ-Al_2O_3 with many sharp peaks was due to the framework ordering. The framework peaks of γ-Al_2O_3 in the XRD pattern of Fe/γ-Al_2O_3 were diminished due to the coverage by iron compounds on its surface. No additional peaks corresponding to ferrous oxide were observed indicating the amorphous nature of the Fe/γ-Al_2O_3 samples.

A high-resolution XPS spectrum of Fe/γ-Al_2O_3 and its iron XPS spectrum are shown in Fig. 3. According to the ratio of the element peak area to the total peak area, the mass percent of Fe, Al and O were estimated to be 0.54%, 29.96% and 69.56%, respectively. Peaks at 710.02 and 720.74 eV in the iron XPS indicated the presence of Fe_2O_3 [18,19], while the peak at 712.03 eV probably implied the presence of FeOOH [20].

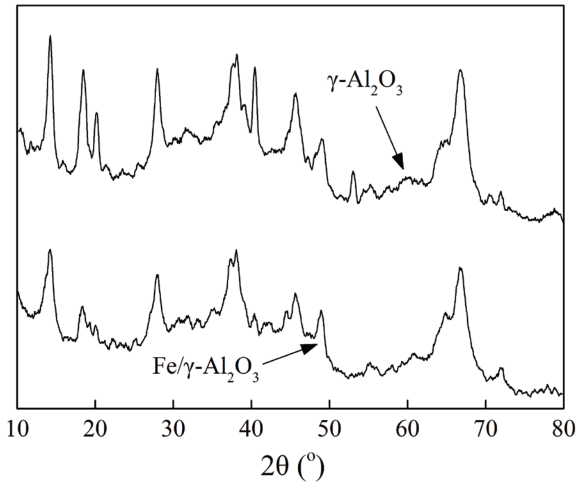

Fig. 2. XRD patterns of γ-Al_2O_3 and Fe/γ-Al_2O_3.

3.2. Effect of initial pH

The initial pH of solution is an important parameter that can significantly affect fluoride adsorption. Fluoride adsorption behavior of Fe/γ-Al_2O_3 under different initial pH was investigated to understand the mechanism of fluoride removal and determine the optimal pH for fluoride removal. The fluoride removal efficiency is shown in Fig. 4, with the pHzpc analysis of Fe/γ-Al_2O_3 particles. As can be seen from Fig. 4, when the initial solution pH (pHi) increased from 1.5 to 5.5; the fluoride removal efficiency increased from 40.82% to 80.66%. A reduction in fluoride removal efficiency from 77.62% to 51.97% was observed with the increase of initial pH from 8.5 to 10.5. The maximum fluoride removal efficiency was observed at the initial pH of 5.5. However, it was interesting to find that fluoride removal efficiency remained almost constant in the initial

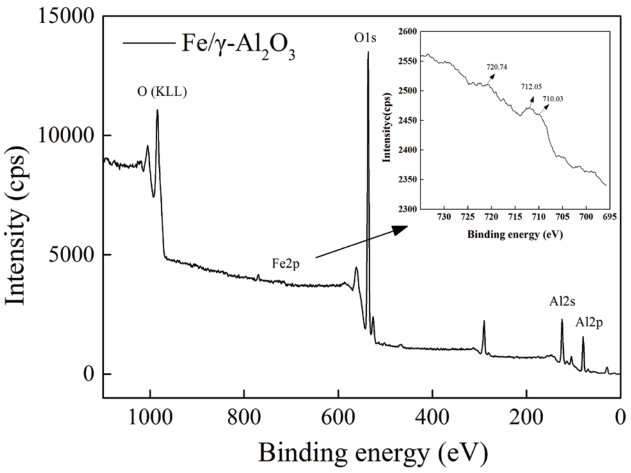

Fig. 3. XPS survey of Fe/γ-Al_2O_3 and the spectrum of Fe2p (inset).

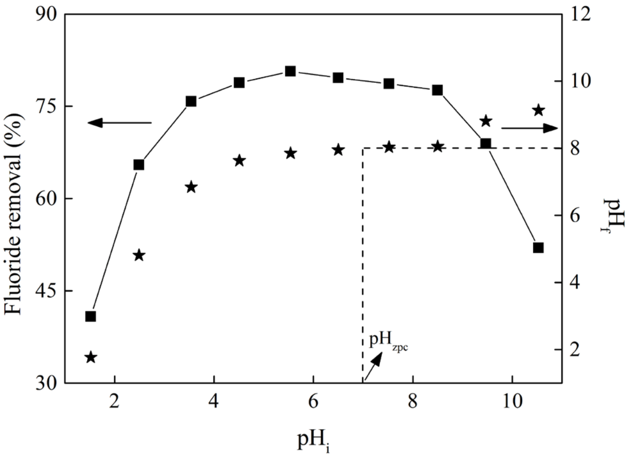

Fig. 4. Effect of initial pH (pHi) variation on fluoride removal and the variation of final pH (pHf) against initial pH (pHi). (adsorbent dose 50 g L^{-1}, initial fluoride concentration 30 mg L^{-1}, equilibrium contact time 24 h and room temperature (25 ± 1°C).

pH range of 4.5–8.5, which is consistent with the pH of natural water environments and beneficial to the application of Fe/γ-Al_2O_3.

Fig. 4 demonstrated the variation of equilibrium pH (pHf) from the pHi during adsorption process. Horizontal portion at pHf ranged 7.95–8.05 should be the pHzpc of prepared adsorbent [3]. Therefore, the surface characteristic of the Fe/γ-Al_2O_3 was (i) positive at pHf < 7.95, (ii) neutral at pHf = 7.95–8.05 and (iii) negative at pHf > 8.05.

It is clear that the Fe/γ-Al_2O_3 exhibited good performance on fluoride removal at pH 4.5–8.0. This can be due to the fact that at pHi < pHzpc, the sorbent surface acquires positive charge which in turn attracts more negatively charged fluoride ion by means of electrostatic interaction. The minimum fluoride removal efficiency at pH < 4.5 can be attributed to the formation of HF and the Al dissolution in the acidic condition due to the complexation of Al and F, which reduced the columbic attraction between fluoride and the adsorbent surface [21,22]. The decrease in fluoride removal efficiency at pH > 8.5 was probably caused by the strong competition of hydroxide ions to the active sites of Fe/γ-Al_2O_3 and also the strong electrostatic repulsion of anionic fluoride by the negatively charged Fe/γ-Al_2O_3 surface. The competition between hydroxyl ions and fluoride for surface sites was also reported with other adsorbent [23–25], such as Fe–Mg–La triple-metal composite [26], Fe/Al mixed hydroxides [1] and Al-doping chitosan–Fe(III) hydrogel [27]. It was also observed from Fig. 4(b) that the pH of the equilibrated solution slightly increased in the acidic pH range while it slightly decreased when the initial solution was alkaline. The reason for this was discussed in the following section.

The above results indicate that the reason for the fluoride removal remaining almost constant in the pH range of 4.5–8.5 can be: (i) Fe/γ-Al_2O_3 had high pHzpc of 7.95–8.05, and the protonation at pH below pHzpc created positively charged surfaces that benefited the removal of fluoride; (ii) in Fe/γ-$Al_2O_{3,}$ the stability of Al species in acidic and alkaline solutions was increased. It is well known that γ-Al_2O_3 can be dissolved to form soluble Al species in either low or high pH conditions. The formation of these soluble Al species decreased the amount of available active sites for fluoride adsorption. Hence, the γ-Al_2O_3 supported by iron changed the Al species distribution on adsorbent and increased the stability of Al species in the range of 4.5–8.5 solutions, which reduced the effect of pH on its removal behaviors toward fluoride. Meanwhile, further research will be carried out to confirm this deduction.

3.3. Effect of co-existing anions

The fluoride-contaminated water may contain several other anions, viz., PO_4^{3-}, SO_4^{2-}, HCO_3^-, NO_3^- and Cl^-. It was possible that these anions would compete with fluoride ions during the adsorption process. Therefore, the effects of these co-existing anions on fluoride adsorption by the Fe/γ-Al_2O_3 adsorbent were examined, and the results were given in Fig. 5. It showed that the presence of SO_4^{2-}, NO_3^- and Cl^- had no significant impact on fluoride adsorp-

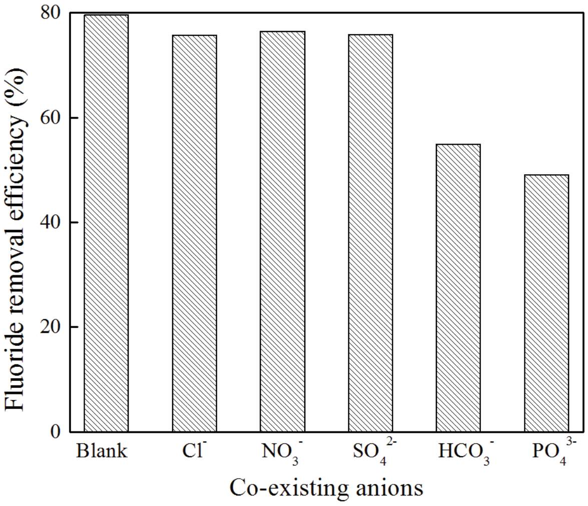

Fig. 5. Effect of co-existing anions on fluoride removal (adsorbent dose 50 g L^{-1}, initial fluoride concentration 30 mg L^{-1}, equilibrium contact time 24 h and temperature 25 ± 1°C).

tion. On the other hand, HCO_3^- and PO_4^{3-} showed some adverse effect. The presence of HCO_3^- decreased fluoride removal efficiency was probably due to the increase of pH after the addition of HCO_3^-. PO_4^{3-} had the most negative effect on the fluoride removal efficiency, which indicated that both the F^- and PO_4^{3-} competed for the same active sorption sites of sorbents and Fe(III) or Al(III) on the adsorbent with higher affinity capacity for P. Similar result has been reported for fluoride removal studies by iron-based materials [3,28,29].

3.4. Adsorption isotherm

The experimental data was obtained at different initial fluoride concentrations and at room temperature. Fig. 6 shows the plots of equilibrium concentration (C_e) vs. fluoride adsorbed per unit mass of adsorbent (q_e).

An adsorption isotherm can be used to acquire the interactional information between adsorbent and adsorbate. The Langmuir and Freundlich isotherm models [30,1] are often used to describe equilibrium adsorption isotherms.

The equilibrium data acquired from isothermal adsorption experiments were analyzed by Langmuir isotherm model and Freundlich isotherm model. The parameters obtained from the analysis of equilibrium data according to Langmuir and Freundlich isotherm models were listed in Table 1. The correlation coefficient (R^2) values of Langmuir isotherm model was higher than those of Freundlich isotherm model, which implied that the isotherm data of the fluoride adsorption on Fe/γ-Al_2O_3 were well fitted to the Langmuir isotherm model. It indicated that a monolayer adsorption was formed on the surface of Fe/γ-Al_2O_3 adsorbent. In the case of fluoride adsorption on plain γ-Al_2O_3, the Freundlich isotherm model gave a higher correlation ($R^2 >$ 0.9975) than the Langmuir isotherm model ($R^2 > 0.9390$). This indicated that multilayer adsorption was involved in the process of fluoride removal by plain γ-Al_2O_3 with heterogeneous surfaces [31].

The Freundlich isotherm model can be adopted to roughly evaluate the adsorption capacity and affinity of an adsorbent toward fluoride. High values of k indicate that an adsorbent has a high adsorption capacity and affinity for fluoride ions. Compared with plain γ-Al_2O_3, the higher value of k was observed for Fe/γ-Al_2O_3 indicating that the former one exhibited higher adsorption capacity for fluoride. The Q_0 values calculated from the Langmuir isotherm model of plain γ-Al_2O_3 and Fe/γ-Al_2O_3 were 1.15 and 1.65 mg g^{-1}, respectively. This suggested that when plain γ-Al_2O_3 was modified with iron, the adsorption capacity for fluoride was improved to a remarkable extent. This can be attributed to the presence of amorphous Fe_2O_3 and FeOOH on the Fe/γ-Al_2O_3 surface that increased the affinity between the Fe/γ-Al_2O_3 surface and fluoride. This was also proved by the results of XRD and XPS analysis.

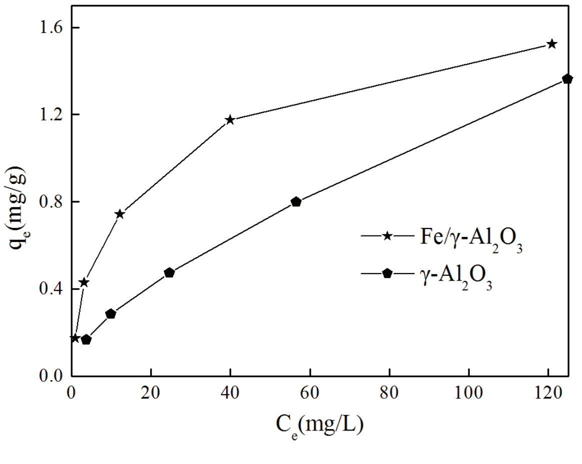

Fig. 6. Adsorption isotherms of γ-Al_2O_3 and Fe/γ-Al_2O_3 for different initial fluoride concentrations (adsorbent dose 50 g L^{-1}, pH 6, contact time 24 h and temperature 25 ± 1°C).

Table 1
Parameters of the Freundlich and Langmuir adsorption isotherm models for fluoride adsorbed by γ-Al_2O_3 samples

Adsorbent	Freundlich			Langmuir		
	k_F	n	R^2	Q_0 (mg g^{-1})	b	R^2
γ-Al_2O_3	0.0744	1.687	0.9975	1.15	0.0359	0.9390
Fe/γ-Al_2O_3	0.2163	2.268	0.9596	1.65	0.0863	0.9948

3.5. Adsorption kinetics

In this study, the fluoride adsorption kinetic was conducted to investigate the adsorption rate. The timing of fluoride adsorption on adsorbent is shown in Fig. 7. It can be seen that fluoride adsorption exhibited an initial rapid uptake within the first 8 h (nearly 80% removal of fluoride); with a further increase in contact time, only a marginal increase of adsorption was observed. After the subsequent 8 h, the fluoride concentration remained constant.

In order to determine the kinetics of fluoride adsorption on the Fe/γ-Al_2O_3 and γ-Al_2O_3 particles, two kinetic models, namely the pseudo-first-order model and the pseudo-second-order model [32,33], were applied to fit the experimental data and explain the solid/liquid adsorption.

The kinetic parameters were obtained from a straight-line fitting of a plot of log (q_e–q_t) against t or a plot of t/q_t against t (Table 2). It was found that for Fe/γ-Al_2O_3, the pseudo-second-order model produced a higher correlation coefficient ($R^2 > 0.998$) than the pseudo-first-order model, which implied that the adsorption of fluoride onto Fe/γ-Al_2O_3 obeyed the pseudo-second-order model for the whole adsorption period, and that the adsorption was a chemically controlled process. It can also be seen that the rate of adsorption for Fe/γ-Al_2O_3 was much faster than that of the plain γ-Al_2O_3.

In adsorption studies, it is necessary to determine the rate-limiting step. Therefore, the results obtained from the experiments were used to study the rate-limiting step in the adsorption process. The amount of fluoride adsorbed per unit mass of adsorbent, q_t at time t, was plotted as a function of square root of time (Fig. 8).

Due to stirring, there is a possibility of transport of fluoride species from the bulk into pores as well as adsorption at the outer surface of adsorbent. It is evident from Fig. 8

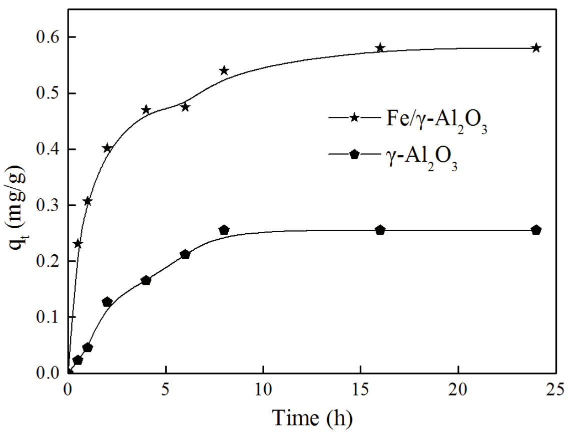

Fig. 7. Effect of contact time the amount of fluoride adsorbed (adsorbent dose 50 g L^{-1}, initial fluoride concentration 30 mg L^{-1}, temperature 25 ± 1°C and pH 6).

Table 2
Kinetic parameters obtained from straight-line fitting of data for the adsorbents

Adsorbent	Pseudo-first-order equation		Pseudo-second-order equation	
	k_1 (1 h^{-1})	R^2	k_2 (g mg^{-1}·h^{-1})	R^2
γ-Al_2O_3	0.2975	0.9817	0.7927	0.9637
Fe/γ-Al_2O_3	0.2529	0.9395	1.5284	0.9988

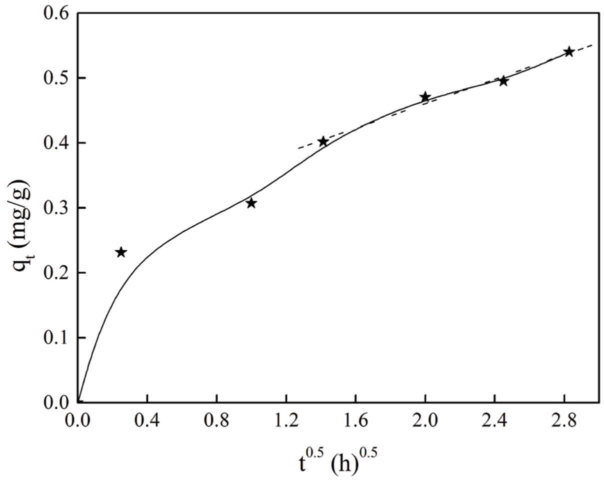

Fig. 8. Plots of amount of fluoride adsorbed vs. $t^{0.5}$ for intra-particle diffusion of fluoride.

that the plot has the features of an initial curved portion and a linear portion. The initial curved portion was attributed to boundary layer diffusion while the linear portion corresponds to intra-particle diffusion [31]. The linear portions of the curves did not pass through the origin in Fig. 8. This indicated that the process of fluoride removal by Fe/γ-Al_2O_3 was complex; both surface adsorption and intra-particle diffusion contributed to the rate-determining step.

3.6. Adsorbent regeneration

The regeneration of exhausted adsorbent is a crucial factor in any sorption process for improving the process economics. In the present study, NaOH solution was used to regenerate the spent adsorbents since its effectiveness has been confirmed by many previous studies [2,11,34]. It was found that the percentages of released fluoride from the exhausted adsorbents were 52.5, 75.8, 81.0, 87.0 and 96.7, when the NaOH solution concentrations of 0.01, 0.05, 0.10, 0.25 and 0.50 M were used to wash the exhausted adsorbents, respectively. The NaOH concentration of 0.50 M was chosen as the optimum desorption reagent for adsorbent regeneration, which can make the 96.7% fluoride release to the solution. The adsorption study was then carried out by using 50 g L^{-1} fluoride-desorbed adsorbents with the initial fluoride concentration of 30 mg L^{-1}. The results showed a sharp decrease in fluoride adsorption efficiency after the regeneration, which may be attributed to the covering of hydroxyl ion on the adsorbent surface during vigorous washing of the adsorbent. Hence, a new recycle protocol was developed to recoat the exhausted adsorbent before reuse. For this, after desorption process using 0.50 M NaOH, the fluoride-desorbed adsorbent was removed from the solution and then washed with weak HCl solutions until the pH value of effluent was neutral. The mixture were dried at 105°C and used for the next adsorption cycle. After the adsorption experiment, it was found that the fluoride adsorption efficiency of regeneration adsorbent was not reduced.

3.7. Proposed mechanism

XRD analysis and XPS analysis have already confirmed that much of amorphous iron oxides were existed on the surface of Fe/γ-Al_2O_3. Surface hydroxyl groups were existed on the surface of amorphous iron oxide [1,27,35] and γ-Al_2O_3 [36]. Therefore, it is speculated that surface hydroxyl groups may be existed on the surface Fe/γ-Al_2O_3 which was composed of hydrated iron oxide and γ-Al_2O_3. The hydrated surface of Fe/γ-Al_2O_3 exhibits an amphoteric behavior in water, which can adsorb or evolve protons. The pH variation during the adsorption of fluoride performed in the effect of solution pH study suggests that surface hydroxyl groups can react with fluoride ion. Combined experimental results and literature, a multiple mechanism for the adsorption of fluoride by Fe/γ-Al_2O_3 was proposed.

The reactions of ionization of the surface hydroxyl groups depend on the solution pH. When the solution is acidic or close to the neutralization, the surface sites of Fe/γ-Al_2O_3 adsorb protons and then show positive charge. The fluoride ions interchange with the surface protonated hydroxyls by the following reactions with the formation of ion pairs with the Bronsted acid site of Fe/γ-Al_2O_3; otherwise, the reaction proceeds with the formation of a complex on the Lewis acid site by ligand exchange.

$$\equiv MOH + H^+ = \equiv MOH_2^+ \ (pH < pH_{ZPC}) \quad (3)$$

$$\equiv MOH_2^+ + F^- = \equiv MOH_2F \quad (4)$$

$$\equiv MOH_2^+ + F^- = \equiv MF + H_2O \quad (5)$$

where M represents metal ion (Fe or Al); ≡MOH represents a surface hydroxyl group and ≡MF a surface site occupied by a fluoride ion.

At pH higher than the pH_{PZC}, the fluoride adsorption on the negative surface of the sample can also be explained by the formation of hydrogen bonds [36] through the interaction with uncharged ≡MOH groups that exist in equilibrium with negative $\equiv MO^-$ groups, as can be seen from Eqs. (6) and (7). At pH above 11, the electrostatic repulsion between the negatively charged surface and fluoride ions exceeds the interaction caused by the formation of hydrogen bonds, which make the adsorption become significantly retarded. The competition between hydroxyl ions and fluoride for the formation of hydrogen bonds on the surface sites may be another reason for the decrease in the adsorption capacity of fluoride.

$$\equiv MOH = \equiv MO^- + H^+ \ (pH > pH_{ZPC}) \tag{6}$$

$$\equiv MOH + F^- = \equiv MOH\cdots F^- \tag{7}$$

The amphoteric behavior of surface hydroxyl groups of Fe/γ-Al_2O_3 can also explain the phenomenon of the pH variation during the adsorption of fluoride. At $pH < pH_{PZC}$, the protons were adsorbed from solution to the surface of Fe/γ-Al_2O_3 because of the protonation reactions, which increased the pH of solution. At basic pH, the decrease in pH of the solution after adsorption was due to surface hydroxyl groups undergoing deprotonation reaction and releasing proton in the aqueous solution.

Compared with γ-Al_2O_3 adsorbent, Fe/γ-Al_2O_3 with higher adsorption capacity and faster adsorption rate can be due to more hydroxyl groups and metal centers with strong affinity toward fluoride ion on the surface of Fe/γ-Al_2O_3.

4. Conclusions

A novel Fe/γ-Al_2O_3-based adsorbent was prepared by a simple Fe(II) impregnation and ultrasonic wave-assisted oxidation method. The BET, TEM, XRD and XPS analysis and the batch adsorption experiment were carried out. The obtained results indicated that the amorphous Fe_2O_3 and FeOOH on the surface of the Fe/γ-Al_2O_3 adsorbent reduced the specific surface area of the adsorbent, but it played an important role in the fluoride adsorption. The prepared absorbent also showed good defluoridation performance. The adsorption capacity calculated from the Langmuir isotherm was 1.65 mg g^{-1}, which was much higher than that of the plain γ-Al_2O_3. For Fe/γ-Al_2O_3, kinetic data were well fitted to a pseudo-second-order kinetic model and the fluoride adsorption rate of Fe/γ-Al_2O_3 which was much faster compared with that of the plain γ-Al_2O_3. The optimum fluoride removal was observed at pH in the range of 4.5–8.5. The presence of bicarbonate and phosphate ions performed extremely negative influence on the fluoride removal while the effect of nitrate ion, chloride and sulfate ions can be negligible. The ultrasonic wave-assisted oxidation method used in this study was proved to be an effective mean to obtain Fe/γ-Al_2O_3 adsorbent with high fluoride removal capacity.

References

[1] M.G. Sujana, G. Soma, N. Vasumathi, Studies on fluoride adsorption capacities of amorphous Fe/Al mixed hydroxides from aqueous solutions, J. Fluorine Chem., 130 (2009), 749–754.

[2] A. Bhatnagar, E. Kumar, M. Sillanpää, Fluoride removal from water by adsorption—a review, Chem. Eng. J., 171 (2011) 811– 840.

[3] N. Chen, Z.Y. Zhang, C.P. Feng, D.R. Zhu, Y.N. Yang, N. Sugiur, Preparation and characterization of porous granular ceramic containing dispersed aluminum and iron oxides as adsorbents for fluoride removal from aqueous solution, J. Hazard. Mater., 186 (2011) 863–868.

[4] A. Tor, Removal of fluoride from an aqueous solution by using montmorillonite, Desalination, 201 (2006) 267–276.

[5] X. Cui, X.D. Wang, W.H. Fan, J.M. Wang, K.Y. Cui, Effects of fluoride on soil properties and yield and quality of maize, Chin. J. Eco-Agriculture, 19 (2011) 897–901.

[6] D.O. Hagan, Fluorine in health care: organofluorine containing blockbuster drugs, J. Fluorine Chem., 131 (2010) 1071–1081.

[7] R.L. Ramos, J.O. Turrubiartes, M.A.S. Castillo, Adsorption of fluoride from aqueous solution on aluminum-impregnated carbon, Carbon, 37 (1999) 609–617.

[8] Ministry of Health of PR China, Standards for drinking water quality, GB5749-2006 (2006).

[9] State bureau of technical supervision of China, Integrated wastewater discharge standard, GB 8978–1996 (1996).

[10] Y.H. Li, P. Zhang, Q.J. Du, X.J. Peng, T.H. Liu, Z.H. Wang, Y.Z. Xia, W. Zhang, K.L. Wang, H.W. Zhu, D.H. Wu, Adsorption of fluoride from aqueous solution by graphene, J. Colloid Interface Sci., 363 (2011) 348–354.

[11] M. Mahramanlioglu, I. Kizilcikli, I.O. Bicer, Adsorption of fluoride from aqueous solution by acid treated spent bleaching earth, J. Fluorine Chem., 115 (2002) 41–47.

[12] P. King, N. Rakesh, S. Beenalahari, Y.P. Kumar, V.S.R.K. Prasad, Removal of lead from aqueous solution using *Syzygium cumini* L.: equilibrium and kinetic studies, J. Hazard. Mater., 142 (2007) 340–347.

[13] T.Y. Datsko, V.I. Zelentsov, Dependence of the surface charge and the fluorine adsorption by γ-aluminum oxide on the solution temperature, Surf. Eng. Appl. Electrochem., 45 (2009) 404–410.

[14] S. Ghorai, K.K. Pant, Investigations on the column performance of fluoride adsorption by activated alumina in a fixed-bed, Chem. Eng. J., 98 (2004) 165–173.

[15] F. Wang, Y. Zhang, M. Yang, J.Y. Cui, Study on adsorption of fluoride ion in drinking water with activated alumina, J. Chin. Agricultural University, 8 (2003) 63–65.

[16] G. Cravotto, P. Cintas, Sonication-assisted fabrication and post-synthetic modifications of graphene-like materials, Chem. Eur. J., 16 (2010) 5246–5259.

[17] B. Tang, J.C. Ge, L.H. Zhuo, G.L. Wang, J.Y. Niu, Z.Q. Shi, Y.B. Dong, A facile and controllable synthesis of γ-Al_2O_3 nanostructures without a surfactant, Eur. J. Inorg. Chem., 21 (2005) 4366–4369.

[18] R.G. Hu, C.J. Lin, XPS/SERS study of electrochemically modified passive film on stainless steel, J. Chin. Soc. Corros. Prot., 20 (2000) 149–154.

[19] H.L. Xiang, W.L. Huang, D. Liu, F.S. He, XPS analysis of corrosion product scale on surface of 29Cr super duplex stainless cast steel, Corros. Sci. Prot. Technol., 23 (2011) 300–312.

[20] X.H. Liu, J. Han, C.Y. Sun, Q.H. Wang, Mechanism of tungstate compound inhibitor in sea water with XPS and EDS, Surf. Technol., 40 (2011) 52–56.

[21] M. Mohapatra, K. Rout, P. Singh, S. Anand, S. Layek, H.C. Verma, B.K. Mishra, Fluoride adsorption studies on mixed-phase nano iron oxides prepared by surfactant mediation-precipitation technique, J. Hazard. Mater., 186 (2011) 1751–1757.

[22] M.G. Sujana, R.S. Thakur, S.B. Rao, Removal of fluoride from aqueous solution by using alum sludge, J. Colloid Interface Sci., 206 (1998) 94–101.

[23] M.G. Sujana, H.K. Pradhan, S. Anand, Studies on sorption potential of some geomaterials for fluoride removal from aqueous solutions, J. Hazard. Mater., 161 (2009) 120–125.

[24] E. Kumar, A. Bhatnagar, M. Ji, W. Jung, S.H. Lee, S.J. Kim, G. Lee, H. Song, J.Y. Choi, J.S. Yang, B.H. Jeon, Defluoridation from aqueous solutions by granular ferric hydroxide (GFH), Water Res., 43 (2009) 490–498.

[25] S.S. Tripathy, J.L. Bersillon, K. Gopal, Removal of fluoride from drinking water by adsorption onto alum-impregnated activated alumina, Sep. Purif. Technol., 50 (2006) 310–317.

[26] Y. Yang, Y. Ling, J.P. Chen, Adsorption of fluoride by Fe–Mg–La triple-metal composite: Adsorbent preparation, illustration of performance and study of mechanisms, Chem. Eng. J., 262 (2015) 839–846.

[27] J.Q. Ma, Y. Shen, C.S. Shen, Y.Z. Wen, W.P. Liu, Al-doping chitosan–Fe(III) hydrogel for the removal of fluoride from aqueous solutions, Chem. Eng. J., 248 (2014) 98–106.

[28] M.G. Sujana, S. Anand, Iron and aluminium based mixed hydroxides: a novel sorbent for fluoride removal from aqueous solutions, Appl. Surf. Sci., 256 (2010) 6956–6962.

[29] Q. Liu, H. Guo, Y. Shan, Adsorption of fluoride on synthetic siderite from aqueous solution, J. Fluorine Chem., 131 (2010) 635–641.

[30] Y. Çengeloğlu, E. Kır, M. Ersöz, Removal of fluoride from aqueous solution by using red mud, Sep. Purif. Technol., 28 (2002) 81–86.

[31] C.Y. Yin, M.K. Aroua, W.M.A.W. Daud, Review of modifications of activated carbon for enhancing contaminant uptakes from aqueous solutions, Sep. Purif. Technol., 52 (2007) 403–415.

[32] Y.S. Ho, G. McKay, Pseudo-second-order model for sorption processes, Process Biochem., 34 (1999) 451–465.

[33] Y.S. Ho, G. McKay, The kinetics of sorption of divalent metal ions onto sphagnum moss peat, Water Res., 34 (2000) 735–742.

[34] M. Streat, K. Hellgardt, N.L.R. Newton, Hydrous ferric oxide as an adsorbent in water treatment: Part 3: batch and mini-column adsorption of arsenic, phosphorus, fluorine and cadmium ions, Process Saf. Environ. Prot., 86 (2008) 21–30.

[35] R.P. Liu, W.X. Gong, H.C. Lan, T.M. Yang, H.J. Liu, J.H. Qu, Simultaneous removal of arsenate and fluoride by iron and aluminum binary oxide: competitive adsorption effects, Sep. Purif. Technol., 92 (2012) 100–105.

[36] T.Y. Datsko, V.I. Zelentsov, Dependence of the surface charge and the fluorine adsorption by γ-aluminum oxide on the solution temperature, Surf. Eng. Appl. Electrochem., 45 (2009) 404–410.